

Monte Carlo study for $\gamma + N \rightarrow \pi + N$ at a new compound target^{*}

ZHANG Yu-Chun(张玉春)^{1,2;1)} LI Yu-Xiao(李玉晓)¹ LI Jia-Cai(李家才)² YU Chun-Xu(喻纯旭)³
CHEN Peng(陈鹏)² WU Yuan-Ming(吴元明)² NIU Wei-Ping(牛卫平)² ZHANG Shao-Ping(张少平)²

¹ (College of Physics and Engineering, Zhengzhou University, Zhengzhou 450052, China)

² (Institute of High Energy Physics, CAS, Beijing 100049, China)

³ (Physical College, Nankai University, Tianjin 300071, China)

Abstract An inbuilt compound target composed of carbon and tungsten is designed, and optimized by realistic GEANT4 Monte Carlo simulation. Also, we do a Monte Carlo study for single-pion photoproduction at the target. The results are presented from the simulation of pion yield, angular distribution and spectrum (at $\theta_{\text{lab}}, \theta_{\text{cm}}=41^\circ$). These efforts are important to the coming measurement of the differential cross section for $\gamma + N \rightarrow \pi + N$.

Key words GEANT4, inbuilt compound target, angular distribution, pion yield, spectrum

PACS 24.10.Lx, 25.20.Lj, 21.60.Ka

1 Introduction

The BEPC II (Beijing Electron Positron Collider) provides an electron beam available at BTF (Beam Test Facility) of IHEP (Institute of High Energy Physics), the maximal energy is 1.89 GeV, and the maximal average intensity is 1.6 A. The experiment of measuring the cross section for single-pion photoproduction at BTF, $\gamma + N \rightarrow \pi + N$, help us to understand the global scaling behavior^[1] at $\sqrt{s}=1.4\text{--}2.1$ GeV. It is a simple process and will bring light for the study of strong interaction. It has larger cross sections at high energy than other exclusive channels due to the slow decrease of the cross sections with energy, i.e., $d\sigma/dt \sim s^{-7}$ ^[2]. In the experiment, high pion production target is required, and pion yield, angular distribution, spectrum (at $\theta_{\text{lab}}, \theta_{\text{cm}}=41^\circ$) and other dynamical properties are also concerned. An inbuilt compound target is designed, and its parameters were optimized through GEANT4 Monte Carlo simulation in this paper.

We use the GEANT4 simulation toolkit^[3] for particle physics and other applications^[4–6]. In addition, the hadronic physics model that is used in the simulation is QGSP_BERT^[7]. This is based on a

Quark-Gluon String model and is recommended by GEANT4 physicist use-case for the majority of the energy range (see details in GEANT4 user's guide^[8]). And the model has successfully been used to simulate pion photoproduction, and the results^[9] agree well with the experimental data. So it is very flexible and has the capability for the calculation and simulation of the complex physical processes of pion photoproduction.

2 An inbuilt compound pion production target

High pion production is very important to single-pion photoproduction. However, simple pion production designed targets are always used as shown in Fig. 1(a)–(c). But these targets have some defects. First, it could not make good use of high energy photons from bremsstrahlung radiator for Fig. 1(b) and Fig. 1(c) especially in the longitudinal direction. From the physical processes of pion from electron striking on target, it is found that the real photon process of pion photoproduction is dominant, because there are two physical processes to produce pion. One

Received 21 March 2008, Revised 30 June 2008

^{*} Supported by National Natural Science Foundation of China (10675138)

1) E-mail: zhangyc@ihep.ac.cn

is virtual photo process of pion photoproduction, the other is real photon process of pion photoproduction. The relationship^[10] between the two processes is:

$$Y_{\text{virtual}}/Y_{\text{real}} = \frac{7t_{\text{eq}}}{9} (t_{\text{eq}} \sim 0.017). \quad (1)$$

Here Y_{virtual} and Y_{real} are pion yield of the virtual and real photon process of pion photoproduction respectively, and t_{eq} is thickness of equivalent radiator. Therefore it could not yield more pions with the same energy and intensity electrons. Second, the pion production target made by liquid LD₂ and ⁴He (see Fig. 1(c)) costs too much, and always needs to be cooled in order to keep temperature steady. Third, for single material target (see Fig. 1(a)), it can be divided into two parts: radiator and pion production target which are made by the same material. As to low Z single material target, the efficiency of radiator is low, while the pion production efficiency is high. Nonetheless, what happens to high Z one is reverse and the energy absorption per pion produced is higher accordingly. Compared with them, the moderate Z target bears hardly any predominance in efficiency of radiator or pion production.

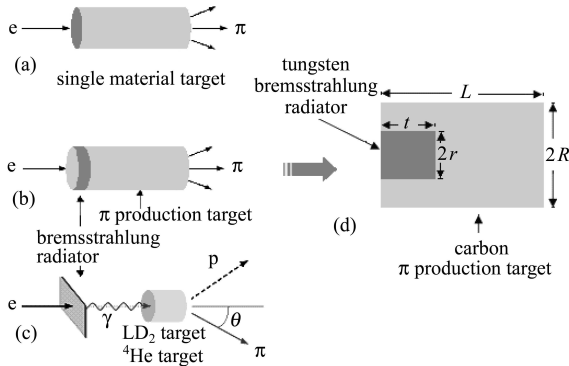


Fig. 1. (a) and (b) show two simple pion production targets used in BTF in the past. (a) is a single material target; (b) is a compound target; (c) schematic view of the experimental pion production target for JLab E94-104^[2]; (d) section plane of the inbuilt compound target, a new design target for BTF.

In order to improve these defects, an inbuilt compound target with tungsten and C-12 is designed. Fig. 1(d) shows a section of the model in the longitudinal direction. It is a cylinder target and has two parts: bremsstrahlung radiator and pion production target; four parameters: r , t , (the radius and the thickness of the radiator), R and L (the radius and thickness of pion production target). And the target will be optimized by changing four parameters in Section 3. High Z material always works as radiator. Tungsten is chosen as the bremsstrahlung radiator.

Because tungsten is a better material working as the bremsstrahlung radiator than copper and iron, it can produce more photons above 1 MeV, and has high melting point (3680 K), and smaller absorption coefficients per radiation length (roughly proportional to $A^{-4/3}$ where A is atomic weight). Low Z material always works as pion production target at lower electron energies (<5 GeV), because of its maximum pion production yield and lower threshold of photonuclear reaction. In addition, low Z materials have low beam energy deposited in the target for a given radiation length because the energy deposition per unit volume is small with low Z low density. Deuterium, beryllium and carbon are three important materials for photonuclear reaction, because of their low threshold. Carbon is the best choice. Carbon target may be ok up to the temperature of 2100 °C. In contrast, the beryllium will be melted at 1278.0 °C. And the nuclear absorption coefficient η per radiation length of carbon is smaller than beryllium's ($\eta_{\text{Be}}=0.375$, $\eta_{\text{C}}=0.234$ ^[11]) for pion. Moreover, the result of GEANT4 simulation shows that carbon cylinder target could produce more pions than beryllium cylinder target with the same parameters and photon energy, as shown in Fig. 2 and Fig. 6 (see details in Section 3.2), even the cross section of beryllium in photonuclear reaction is larger than carbon's. As to deuterium target, it has no attraction for us because of its high cost and complicated cool system.

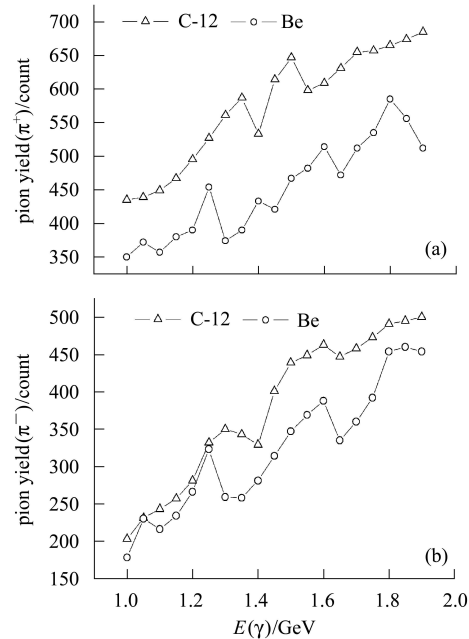


Fig. 2. π^+ (a) and π^- (b) yield as a function of photon energies (1—1.9 GeV) with the same parameters of two cylinder targets (carbon and beryllium).

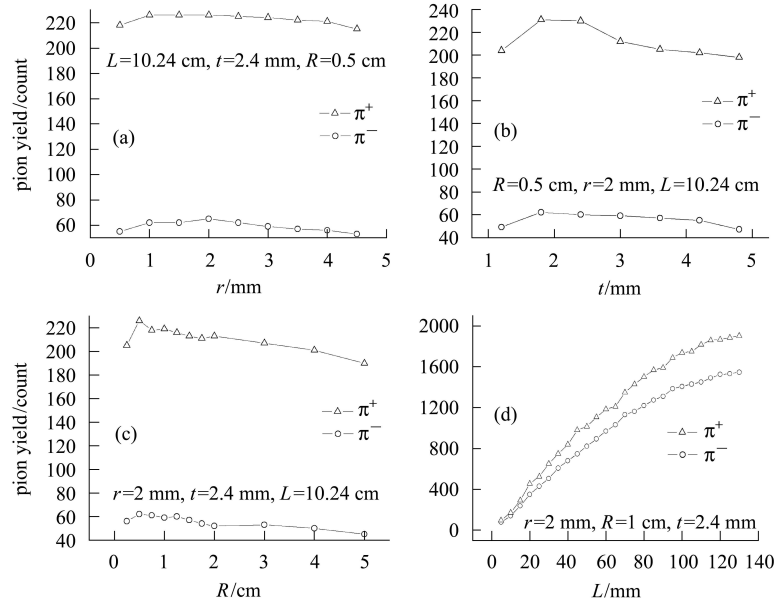


Fig. 3. Pion yields versus the parameters (r , t , R , L) of compound target at $E(e^-)=1.6$ GeV.

3 Optimization of the inbuilt compound target and GEANT4 simulation

3.1 Optimizing the inbuilt compound target

As the inbuilt compound target has been designed, it can be optimized by changing its parameters (r , t , R , L) in order to get appropriate pion yield. In this section, pion yields depending on the parameters of the compound target will be studied respectively. The pion yields as the function of the parameters values are shown in Fig. 3(a)—(d). It can be observed that the pion yields approach the maximum at $r=2$ mm, $R=0.5$ cm when other parameters are fixed. From Fig. 3(d), it can be found that the number of pions increases when the thickness of target increases, but the increasing rate of the number decreases. We always choose the thickness of carbon target to be approximately 100 mm. Because if the target is too thick, the more energy of pion will deposit in target although the pion yield also increases. As to the thickness of radiator, Y. S. Tsai and van Whitis^[11] point out that practically all the high-energy photons are produced by radiator from $t=0$ to $t=0.75rl$ (t is the thickness of radiator, rl is radiation length), and after $t=0.75rl$, the intensity of the photon is attenuated by the absorption factor $e^{-7/9(t-0.75)}$. Intensity of the photons whose $k/E_e > 0.75$ (k is the energy of first generation photon, E_e is the energy of incident electron) will be maximal at $t=2.4$ mm ($t=0.69rl$, $1rl=3.5$ mm for W). And the pion yield reaches maximum almost in all the regions of incident electron energy at $t=2.4$ mm when other parameters are fixed, as shown in Fig. 4 by GEANT4 simulation,

even it is not obvious in Fig. 3(b). As discussed above, the pion yield of the target is comfortable (the pion yield is higher, and the energy absorption of pion is smaller) at $r=2$ mm, $R=0.5$ cm, $t=2.4$ mm ($0.69rl$), $L=102.4$ mm. In addition, pion spectrum of the inbuilt compound target is shown in Fig. 5. From the picture, we find that pion yield shows some oscillating characteristic, especially in π^+ spectrum, which indicates there are abundant hadron-resonances in the

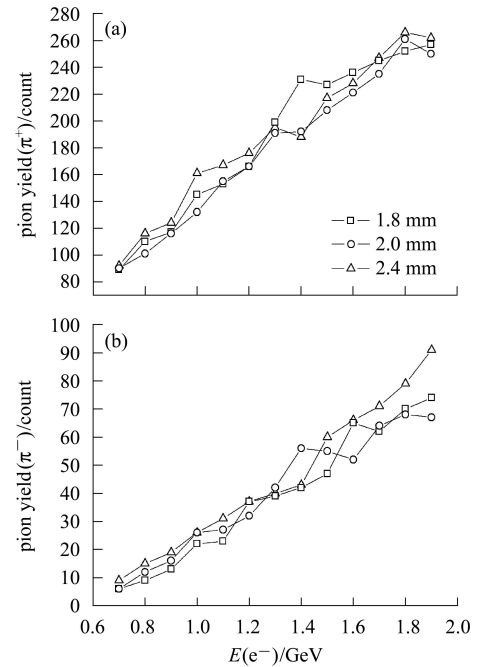


Fig. 4. The detailed comparison of pion yield between $t=1.8$ mm ($0.514rl$), 2 mm ($0.57rl$) and 2.4 mm ($0.69rl$) when other parameters fixed at $r=2$ mm, $R=0.5$ cm, $L=102.4$ mm respectively and (a) is for positive pions and (b) is for negative pions.

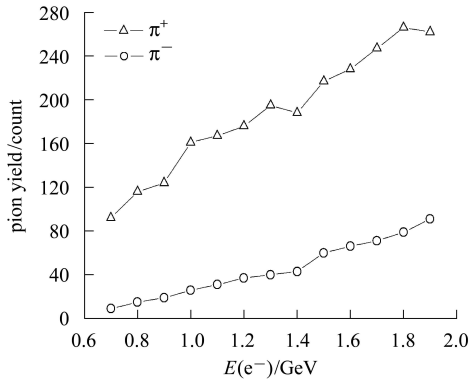


Fig. 5. Pion (π^+ and π^-) yield versus incident electron energies (0.7—1.9 GeV) for the optimized compound (W/C) target at $r=2$ mm, $R=0.5$ cm, $t=2.4$ mm (0.69rl), $L=102.4$ mm.

energy region ranging from 0.7 to 1.9 GeV. In addition, the ratio of positive pions to negative pions is larger than 1.

3.2 Comparison of simulation results with other targets

We have also optimized other different material targets in the same way: a single material cylinder carbon target ($R=0.5$ cm, $L=102.4$ mm), a single material cylinder beryllium target ($R=2$ cm, $L=102.4$ mm), another inbuilt compound cylinder target is made up of tungsten and beryllium ($R=2$ cm, $L=102.4$ mm, $t=1$ mm, $r=2$ mm). And Fig. 6 shows the results of the simulation with the incident electron beam energy in the range from

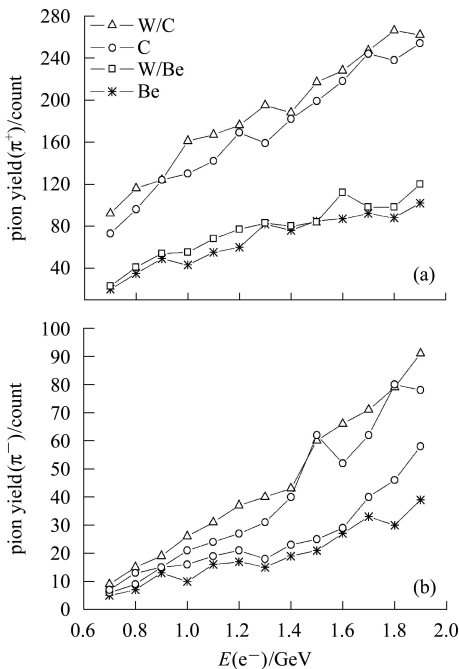


Fig. 6. π^+ (a) and π^- (b) yield versus incident electron energies (0.7—1.9 GeV) for different material targets.

0.7 GeV to 1.9 GeV. Comparing the simulation results of four different material targets, we find that the W/C inbuilt compound target performs better than others. Because the pion (positive and negative) that yields from the W/C target is larger than other targets almost in all the region of incident electron energy, therefore the inbuilt compound target has more advantages compared with single material target.

4 Pion angular distribution and spectrum at $\theta_{lab}, \theta_{cm} = 41^\circ$

4.1 Pion angular distribution

Pion angular distribution is an interesting feature in the single-pion photoproduction experiment. The off-axis angle of the outgoing pion with respect to the Z axis of the target will be studied. The pion distribution calculated using GEANT4 by 1.8 GeV incident electron beams is plotted in Fig. 7. From the plot, we see that the counts of π^+ are approaching maximum approximately at $\theta=33^\circ$ in contrast to $\theta=39^\circ$ for π^- . As electron beam energy ranges from 1 GeV to 1.9 GeV, there exist unobvious changes regarding the angular distribution. It is very important to us for choosing the position and angle of received system.

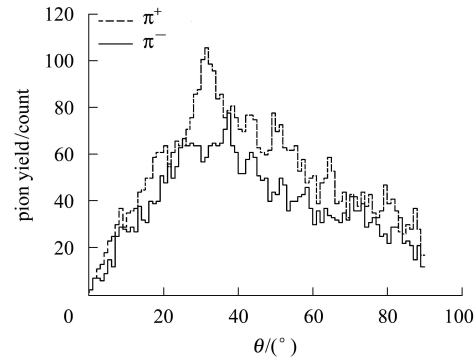


Fig. 7. Pion angular distribution from the inbuilt compound target with incident 1.8 GeV electron beam.

4.2 Pion spectrum at $\theta_{lab}, \theta_{cm} = 41^\circ$ respectively

The next interesting point is pion spectrum at fixed angle: pion yield at $\theta_{lab}, \theta_{cm}=41^\circ$ versus incident electron beam energy at the optimized inbuilt compound target. The electron energies range from 0.6 GeV to 1.9 GeV, corresponding to center-of-mass energies from 1.41 GeV to 2.11 GeV by using a photon energy close to the incident electron beam energy just like in Ref. [2], as shown in Fig. 8. From the plot, it can be seen that pion yield at $\theta_{cm}=41^\circ$ is larger than that at $\theta_{lab}=41^\circ$, no matter what kinds of pion it is.

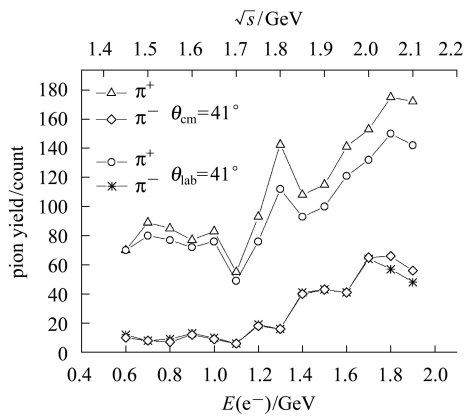


Fig. 8. Pion spectrum at $\theta_{lab}=41^\circ$ and $\theta_{cm}=41^\circ$ from the inbuilt compound target with the incident electron beam energies ranging from 0.7 GeV to 1.9 GeV, corresponding to the center-of-mass energies (\sqrt{s}) from 1.41 GeV to 2.11 GeV for $\gamma+N \rightarrow \pi+N$.

In addition, pion spectrum has some oscillation which may exhibit the oscillation of the differential cross

section around the scaling value predicted by CCR^[2] (Constituent Counting Rule).

5 Conclusion

A cylindrical inbuilt compound target composed of tungsten and carbon has been optimized with Monte Carlo simulation. The target not only has higher pion production, but also has the features of heat-resistance and lower energy deposit. In addition, the pion yield and angular distribution are also studied. Moreover, the pion spectrum at $\theta_{lab}, \theta_{cm}=41^\circ$ exhibits oscillation. These results in the paper are important to the coming measurement of the differential cross section for $\gamma+N \rightarrow \pi+N$ and update of BTF.

We would like to thank Dr. Xu Xin-Ping (Huazhong Normal University and Experiment Physic Center of IHEP) for his many inspiring discussions.

References

- Schulte E C et al. Phys. Rev. Lett., 2001, **87**: 102302; Freedman S J et al. Phys. Rev. C, 1993, **48**: 1864; Belz J E et al. Phys. Rev. Lett., 1995, **74**: 646; Napolitano J, Mirazita M et al. Phys. Rev. C, 2004, **70**: 014005
- ZHU L Y, Arrington J et al. Phys. Rev. Lett., 2003, **91**: 2; ZHU L Y, Arrington J et al. Phys. Rev. C, 2005, **71**: 044603
- <http://geant4.web.cern.ch/geant4/>
- Allison J et al. IEEE Trans Nucl Sci, 2006, **53**(1): 270—278
- Geant4 Collaboration. <http://geant4.web.cern.ch/geant4,> 2006, September
- Agostinelli S et al. Nucl. Instrum. Methods Phys. Res. A, 2003, **506**: 250—303
- [http://www/geant4.org/geant4/support/proc_modcatalog/physicsists/referencePL.shtml](http://www.geant4.org/geant4/support/proc_modcatalog/physicsists/referencePL.shtml)
- <http://geant4.web.cern.ch/geant4/UserDocumentation/UsersGuides/PhysicsReferenceManual/html/node133.html>
- <http://geant4.web.cern.ch/geant4/support/userdocuments.shtml>
- Tsai Yung-Su. Review of Modern Physics, 1974, **46**: 815—851
- Tsai Y S, van Whitis. Phys. Rev., 1966, **149**: 1248—1257